SAND2006-3363C

# Microstructural Features in Aged Erbium Tritide Foils

**D. S. Gelles[1], L. N. Brewer[2], P. G. Kotula[2], D. F. Cowgill[3], C. C. Busick[2] and C. S. Snow[2]**

**[1] Pacific Northwest National Laboratory, Richland, WA 99352**
**[2] Sandia National Laboratory, Albuquerque, NM 87185-0886**
**[3] Sandia National Laboratory, Livermore, CA 94551-0969**

**To be submitted for consideration as part of the proceedings of the 23rd ASTM International Symposium on Effects of Radiation on Materials to be held June 13-15, 2006 in San Jose, California.**

# Microstructural Features in Aged Erbium Tritide Foils

**D. S. Gelles[1], L. N. Brewer[2], P. G. Kotula[2], D. F. Cowgill[3], C. C. Busick[2] and C. S. Snow[2]**

**[1] Pacific Northwest National Laboratory, Richland, WA 99352**
**[2] Sandia National Laboratory, Albuquerque, NM 87185-0886**
**[3] Sandia National Laboratory, Livermore, CA 94551-0969**

## Abstract

Aged erbium tritide foil specimens are found to contain five distinctly different microstructural features. The general structure was of large columnar grains of $ErT_2$. But on a fine scale, precipitates believed to be erbium oxy-tritides and helium bubbles could be identified. The precipitate size was in the range of ~10 nm and the bubbles were of an unusual planar shape on {111} planes with an invariant thickness of ~1 nm and a diameter on the order of 10 nm. Also, an outer layer containing no fine precipitate structure and only a few helium bubbles was present on foils. This layer is best described as a denuded zone which probably grew during aging in air. Finally, large embedded $Er_2O_3$ particles were found at low density and non-uniformly distributed, but sometimes extending through the thickness of the foil. A failure mechanism allowing the helium to escape is suggested by observed cracking between bubbles closer to end of life.

## Introduction

Erbium provides a useful storage medium for tritium. However, with time, the tritium decays to $^3He$ with the release of a $\beta^-$ particle (half life of 12.33 yrs.) according to the reaction

$$^3H \rightarrow \beta^- + {}^3He$$

The $^3He$ atoms initially occupy interstitial sites, but are mobile at room temperature, and can cluster, growing to become helium bubbles, and escape. The release rate, and variation in release rate of $^3He$ as a function of sample dimension is of interest. Recent efforts to quantify and model helium bubble development in tritides has resulted in the need for detailed microstructural information.[1] This report is intended to document microstructural examination results on several erbium tritide foils in order to define the important features found in such foils.

## Experimental details

Erbium tritide coatings are created by vapor deposition of erbium metal on annealed molybdenum substrates. The coatings are subsequently tritided. Coatings are as thick as 500 nm, but the purpose of the present work was to evaluate coatings of various thicknesses. The tritide coatings on molybdenum substrates were prepared for transmission electron microscopy in cross section using standard ion milling procedures with a Gatan Precision Ion Polishing System (PIPS) in the tritium envelope at SNL-NM. This allows examination of the full cross section of the coating tilted on edge. Examinations were performed on a JEOL 2000FX equipped with a digital camera and an EDAX x-ray spectrometer in that facility.

## Results

The foil specimens that were examined are summarized in Table 1, listed in order of examination date. Table 1 includes aging information showing that all but two of the conditions were aged ~4 years whereas specimen 3329003 was aged only 10 months and 3319010 was aged 1 year. Age is defined as the time from tritiding to examination following preparation.

Table 1. Specimen conditions examined.

| ID | Sample Age (years) | Foil Thickness (nm) | ~Denuded Zone Thickness (nm) |
|---|---|---|---|
| 4277-05 | 3.5 | 500 | 40 |
| 3143006 | 2.75 | 200 | 20 |
| 3329003 | 0.83 | 500 | 10 |
| 3162016 | 4.25 | 100 | 10 |
| 3139007 | 4.25 | 100 | 13 |
| 3319010 | 1.0 | 500 | 17 |
| 3147001 | 5.0 | 300 | 25 |

Microstructures found in all specimen conditions were similar. The general structure was of large columnar grains of erbium tritide ($ErT_2$) probably on the order of 1 μm in diameter that showed a distinct mottled appearance on a scale of ~10 nm. This columnar microstructure is consistent with the crystallographically textured nature of the films as has been shown previously by x-ray diffraction. [2] The mottling is due to precipitation, as indicated by extra spots in diffraction patterns and dark field imaging. However, the external edge of foils showed a band of material ~10-40 nm thick which did not have this mottled appearance; we describe it as a denuded zone. When specimens could be suitably oriented, unusual bubbles or "cavities" were observed. The cavities were planar, lying on {111} planes. They ranged in diameter from 5 to 25 nm, but with a uniform thickness of ~1.0 nm. These planar cavities were also identified by Bond etal [3] when they had the opportunity to examine similar material. Larger, more complex bubble or crack shapes decorated columnar grain boundaries. Occasionally, grains were found within the foil that did not show mottling. These regions were sometimes found extending through the full thickness of the foil. Analysis of x-ray spectroscopy and electron diffraction patterns from these regions matched $Er_2O_3$ indicting that these grains are oxide particles. Therefore, five distinct features are 1) the base structure $ErT_2$ in the form of large columnar grains, 2) coherent fine precipitates distributed within the erbium tritide, 3) a surface denuded zone on the erbium tritide, 4) planar helium bubbles lying on {111} planes with larger bubbles or cracks on columnar grain boundaries, and 5) large particles of erbium oxide embedded in the erbium tritide.

Examples of these features are provided in figures 1 to 3. Figure 1 for condition 3143006 shows an erbium tritide foil in cross section laid down on a molybdenum substrate at the left. Bubbles or cracking at a columnar grain boundary, bubbles edge-on on a {111} plane and a denuded zone at the external surface are labeled. Bubbles on a second set of {111} planes can also be identified nearly edge-on for this foil which is near an <011> orientation, with the two sets approximately 70º apart. Note that the bubbles edge-on appear very uniform in thickness, independent of diameter and that those not quite edge-on have finite width demonstrating planar, as opposed to rod, geometry. The upper grain is near a different (011) orientation, so that bubbles at the upper left are not aligned with bubbles in the lower grain. Figure 2 gives a second view of the specimen after slight tilting so that a second bubble orientation is more clearly shown, along with a weak beam dark field image using g=111 with a large aperture, and a typical (011) diffraction pattern . As the bubbles do not appear in dark field images, it is likely that a precipitate spot is responsible for the contrast observed and this is the precipitate responsible for extra spots showing in the diffraction pattern inset. Diffraction patterns such as this showed no Kikuchi structure, indicating significant strain results from the

presence of either the precipitate particles or stored $^3$He. Figure 3 shows analysis for a large oxide particle in condition 3329003. A view of the particle in the erbium tritide is shown in a) and the <110> zone axis diffraction pattern with indexing is given in b) and c). X-ray spectroscopy indicates this is an oxide, corroborated by planar spacing measurements. However, it should be noted that although the diffraction information shows a match to $Er_2O_3$ it appears to have a systematically smaller lattice parameter by ~0.2Å.

The range of response for the conditions examined is shown in Figure 4. The images selected show one set of {111} bubbles on edge. However, the bubble images for condition 4277-05 which was examined early in our study, are much broader. It has been found when comparing bubble images in thinner areas with those in thicker areas, that bubbles were much broader in thin areas. This observation is understood to be due to an ion milling artifact resulting when planar bubbles intersect specimen surfaces, caused by enhanced milling at the resulting oblique surfaces compared to the glancing angle of the general surface. Therefore, differences in bubble width for condition 42- should be ignored because the area examined was probably too thin. From Figure 4, it can be demonstrated that all samples developed planar helium bubbles, but the sizes and apparent number densities do not follow a simple progression on aging time or film thickness.

An example was found in sample 4277-05 where bubble platelets were incorporated into the denuded zone, shown in Figure 5. Therefore, the process which creates the denuded zone does not remove the helium bubbles. Table 1 includes estimates of denuded zone thickness for conditions examined. However, no simple progression can be demonstrated between denuded zone thickness and aging time or film thickness.

A possible failure mechanism can be envisioned based on cracking between bubbles. The example is provided from sample 4277-05 in Figure 6 showing a region containing helium bubbles with a crack visible linking four bubbles in the upper part of the micrograph. This image was taken in an under-focused condition, which can show such cracks clearly. Therefore, as bubbles grow, cracks between bubbles can develop, eventually allowing cracking to reach the surface.

It was possible to estimate sample thickness from stereo information for most specimen conditions in order to quantify bubble information. Bubble diameter and bubble density estimates are provided in Table 2, with results of bubble density from one set of planar bubbles multiplied by four to estimate total bubble density. Table 2 has been organized in increasing sample age, and it can be shown that no simple progression of bubble size can be demonstrated. This is in disagreement with preliminary results by Bond etal [3] as noted above where bubble diameter was found to increase with increasing aging time.

Table 2. Quantification measurements

| ID | Sample Age (yrs) | Film Thickness (nm) | ~Denuded Zone Thickness (nm) | Bubble Diameter (nm) | Bubble Density* (#/cm3) |
|---|---|---|---|---|---|
| 3329003 | 0.83 | 500 | 10 | na | na |
| 3319010 | 1.0 | 500 | 17 | 2.0 ± 0.8 | $2.4 \times 10^{17}$ |
| 3143006 | 2.75 | 200 | 20 | 12.3 ± 4.9 | $3.2 \times 10^{17}$ |
| 4277-05 | 3.5 | 500 | 40 | na | na |
| 3162016 | 4.25 | 500 | 10 | 8.3 ± 0.9 | $2.9 \times 10^{17}$ |
| 3139007 | 4.25 | 100 | 15 | 3.6 ± 0.8 | $9.1 \times 10^{17}$ |
| 3147001 | 5.0 | 300 | 25 | 15.4 ± 7.2 | $7.9 \times 10^{16}$ |

* Corrected to include four variants.

## Discussion

Bubbles

Planar helium bubbles in materials are unusual, but several examples have been previously observed. Planar helium bubbles have been found in molybdenum,[4] nickel,[5] boron carbide,[6] and silicon carbide.[7] In Ni, $B_4C$ and $ErT_2$, the bubbles form on (111) planes but in α-SiC, the habit plane is (0001) and in bcc Mo, bubbles form on (110) planes. Bubble thicknesses are often invariant with size, for $B_4C$, 4 nm, for $ErT_2$ ~1 nm, for Mo <1 nm and SiC ~0.6 nm, but poorly defined for Ni, probably ~1 nm. Therefore, our observations of planar helium bubbles are similar to these other examples.

The planar bubbles can be expected to contain helium in a condensed state. It is possible that the bubble shape arises because the helium is in a solid form and therefore the helium bubbles can be thought of as precipitates, but calculations indicate that the phase should be liquid. It was not possible to obtain diffraction information from the bubbles.

Our observation that bubble size did not correlate with aging time requires explanation. With aging time, helium levels increase. Therefore, either bubble size or density must increase, whereas Table 2 does not demonstrate such a trend. The discrepancy can probably be trace to statistical uncertainty arising either from too small a sample size or from the assumption that the total bubble populations can be estimated based on measurements from only one of the four {111} populations. Sample size was limited by the nature of the films in cross section and the limited area obtained for examination by ion milling. As a result, measurements are based on tens of bubbles. Bond [3] used an ion milling preparation procedure so the film was thinned to electron transparency through the thickness and therefore, much larger bubble populations were available for measurement. It is also possible that in a given area of interest, bubbles are not uniformly distributed on the various {111} planes. As bubble imaging is most effective with the bubbles edge on, a great deal of effort is needed to observe three sets in an area of interest and no attempt was made. In the case of BC,[6] bubble clustering was observed, suggesting that in a given area, certain of the {111} orientations was preferred. The Bond samples were always in the plane of the molybdenum support, so any preferential rafting would always appear invariant.[6] Therefore, our apparent lack of correlation may have arisen from limited statistics or an invalid assumption that populations should be uniformly distributed on the available planes.

Denuded zone

It was not possible for us to obtain denuded zone composition information due to electron beam limitations in the JEOL 2000FX. However, J. A. Knapp was able to make use of heavy ion elastic recoil detection (ERD) using a 28 MeV $Si^{+4}$ ion beam to show that the outer layer of $ErT_2$ about 10 nm thick contains enrichment of oxygen.[4] This thickness is in good agreement with denuded zone measurements in our specimens. Therefore, it is reasonable to expect that the denuded zone is a result of oxidation. However, the quantitative behavior we obtained does not correlate with aging time as might be expected. In general, $ErT_2$ samples are kept under vacuum. The oxidation process can be successfully slowed by storage in a reduced oxygen environment, so that oxidation only occurs when the samples are removed from vacuum for specimen preparation procedures. Therefore, the denuded zone thickness is probably a measure of the time a sample is out of vacuum

during cross section specimen preparation, and we were probably least efficient at specimen preparation on the first attempt with specimen 4277-05.

Fine precipitate particles

If indeed the denuded zone forms as a result of oxygen enrichment, it is likely that the fine background precipitate is oxygen rich, because it becomes invisible in the denuded zone regions where more oxygen has been introduced. Then this fine precipitate would arise as a result of oxygen left in solution after the evaporation process. It can be anticipated that this precipitation markedly hardens the tritide. If it could be eliminated, it may lead to improved mechanical properties in the tritide and longer helium retention because ligaments between bubbles would be tougher.

Large oxide particles

Larger oxide particles are present in $ErT_2$ foils. For both larger and fine oxygen-containing particles to be present, it is expected that they must form at different times during processing. We therefore theorize that the large particles formed during the erbium evaporation process or a subsequent high temperature anneal, whereas the fine precipitates grew during annealing of the $ErT_2$ at room temperature, absorbing the remaining oxygen in solution. The reduced lattice parameter observed in the larger oxide particles probably arises because of the incorporation of tritium into the lattice perhaps reducing the oxygen level below stoichiometry and providing more oxygen to the $ErT_2$ matrix.

## Conclusions

Erbium tritide films have been characterize as a function of film thickness and aging time. It is found that typical films contain five distinct features: large columnar grains of $ErT_2$, planar helium bubbles on {111} planes with an invariant thickness of ~1 nm and diameters in the range of ~10 nm at densities of $0.8\text{-}9\text{x}10^{17}$ $cm^{-3}$ but with larger bubbles on grain boundaries, a fine precipitate in the size range of ~10 nm believed to be erbium oxide pobably containing tritium, an outer layer containing no fine precipitate structure and only a few helium bubbles with a thickness of 10-40 nm and believed to be erbium oxide probably containing tritium which grew during aging in air, and large embedded $Er_2O_3$ particles at low density and non-uniformly distributed, but sometimes extending through the thickness of the foil that were possibly present prior to tritiding. Attempts to quantify bubble sizes and densities were probably impaired by insufficient statistics.

## References

[1] D. F. Cowgill, "Helium Nano-Bubble Evolution in Aging Metal Tritides," Sandia Report SAND 2004-1739 (2004).
[2] M. Rodriguez, "X-ray and Neutron Diffraction of Er-Hydride Films," presented at the Working Group on the Physics and Chemistry of Metal Tritides, October 13, 2004, Albuquerque, NM.
[3] G. Bond, J Browning and E Schmidt, "Microstructural Development in Model $ErT_2$ Films," presented at the Working Group on the Physics and Chemistry of Metal Tritides, October 13, 2004, Albuquerque, NM.
[4] J. E. Evans, A. Van Veen and L. M. Caspers, Nature 291, (1981) 310-312 or A. Van Veen and L. M. Caspers and J. E. Evans, J. Nucl. Mater., 103 & 104 (1981) 1181-1186.
[5] M. D'Olieslaeger, L. deSchepper, G. Knuyt and L. M. Stals, J. Nucl. Mater., 138 (1986) 27-30.

[6] A. Jostsons, C. K. H. DuBose, G. L. Copeland and J. O. Stiegler, , J. Nucl. Mater., 49 (1973-74) 136-150.
[7] J. Chen, P. Jung and H. Trinkaus, Phys. Rev. Letters, 82 (1999) 2709-12 or Phys. Rev. B 61 (2000) 12 923-932

Sandia is a multiprogram laboratory operated by Sandia Corporation, a Lockheed Martin Company, for the United Stated Department of Energy (DOE) under contract DEAC0494AL85000.

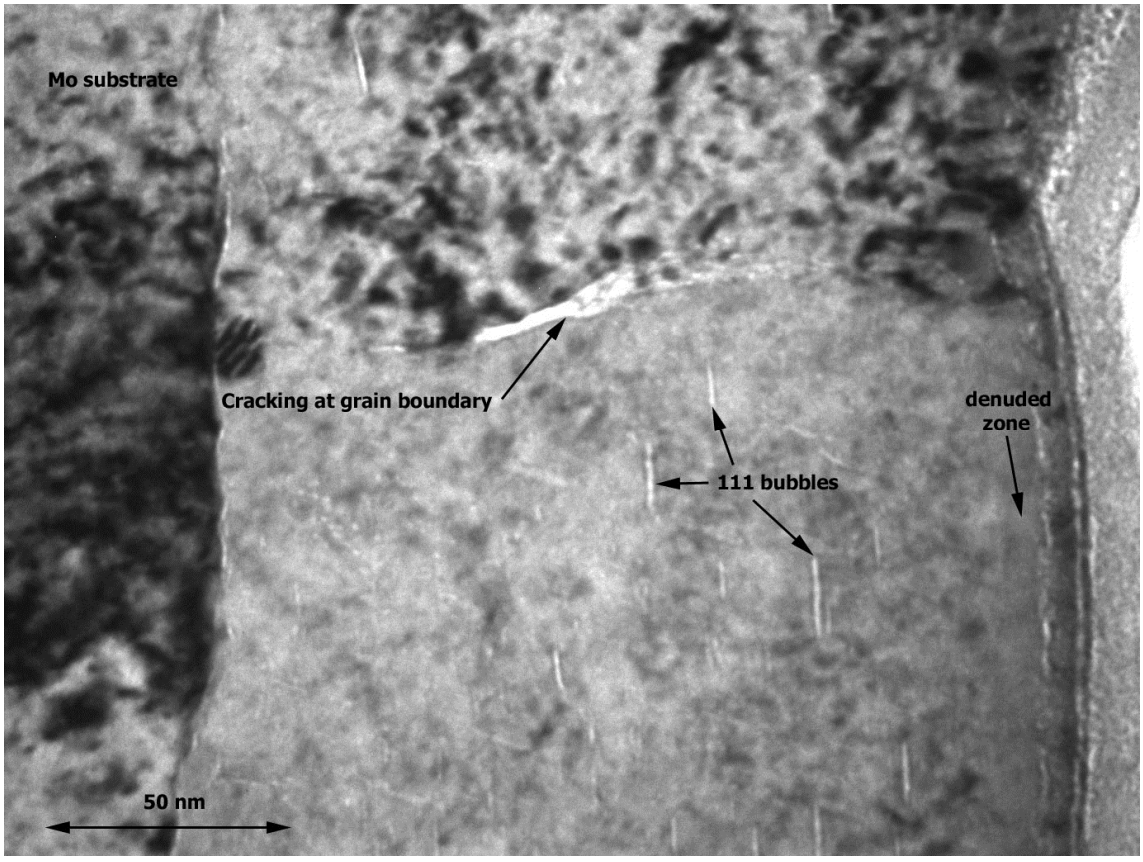


Figure 1. Erbium foil in specimen 3143006. Bubbles on two sets of {111} planes, cracking at a grain boundary and a surface denuded zone are identified in the foil along with the Mo substrate.

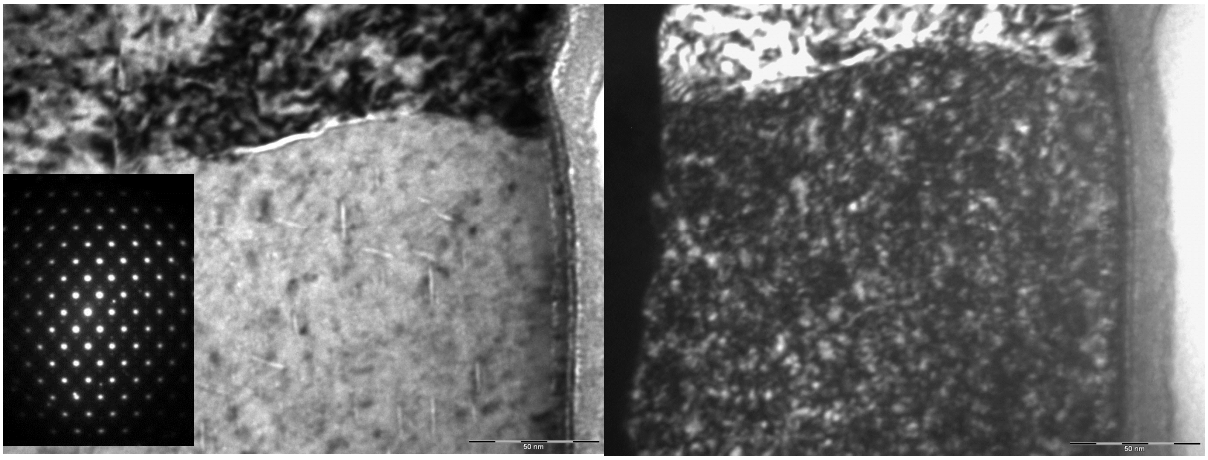

Figure 2. Bright and dark-field (g=111) images are shown for specimen 3143006 with a typical selected area diffraction pattern inset. A second set of {111} cavities and evidence for precipitation can be seen.

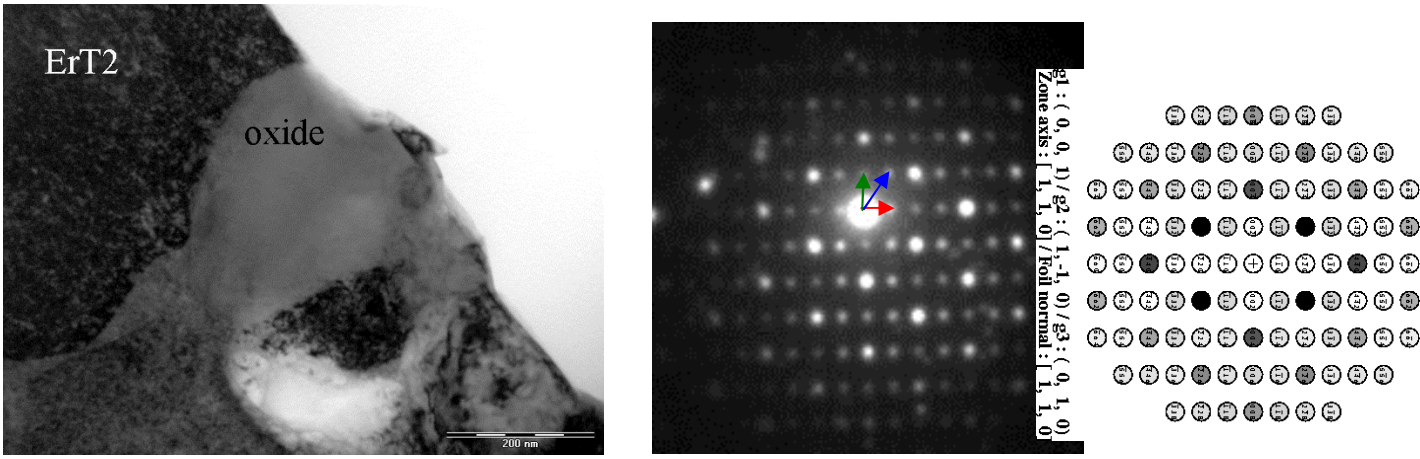


Figure 3. A large oxide particle in Specimen 3329003, a selected area diffraction pattern in <110> orientation, with accompanying indexing for $Er_2O_3$.

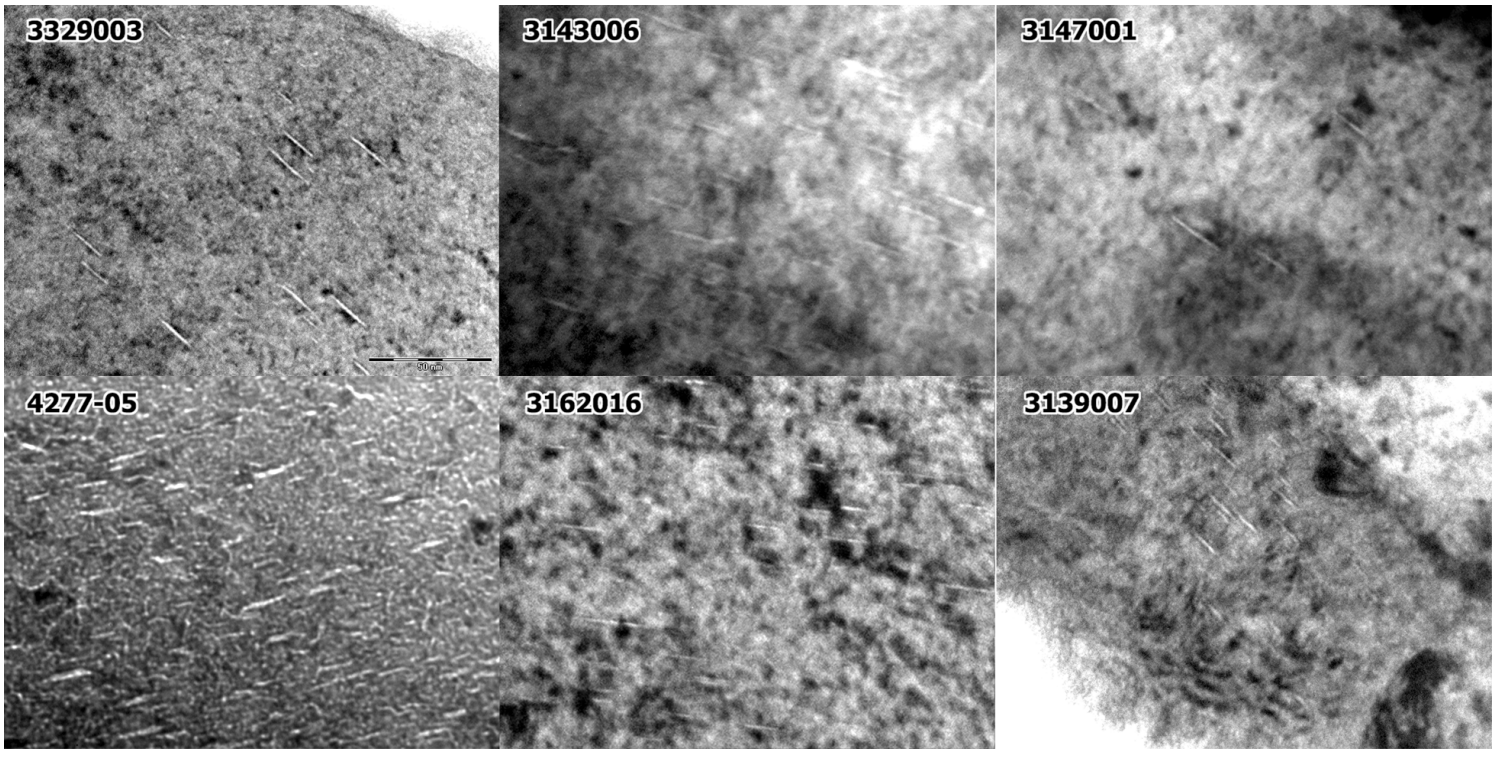


Figure 4 Examples of He bubbles in a) 3329003, b) 3143006, c) 3147001, d) 4277-05, e) 3162016 and f) 3139007.

Figure 5. Denuded layer in specimen 4277-05 showing helium bubbles retained within the layer.

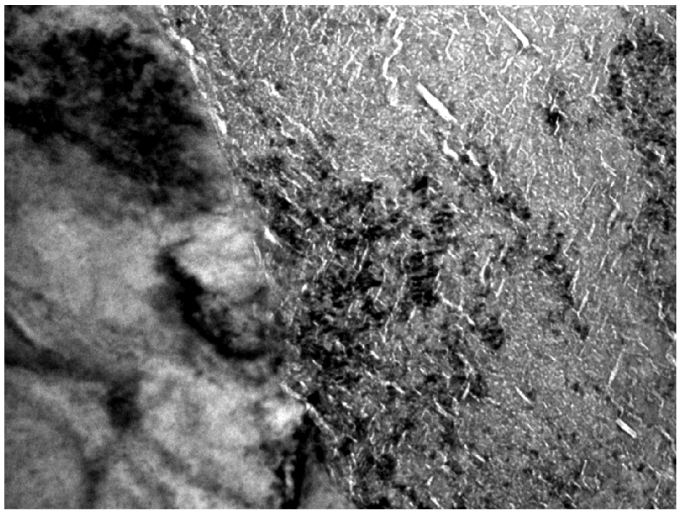

Figure 6. Helium bubbles in specimen 4277-05 showing a crack linking four bubbles at the top.